# Robust symmetric patterns in the Faraday experiment

R. A. Barrio, J. L. Aragón, and C. Varea
*Instituto de Física, Universidad Nacional Autónoma de México, Apartado Postal 20-364, 01000 México, Distrito Federal, Mexico*

M. Torres, I. Jiménez, and F. Montero de Espinosa
*Instituto de Física Aplicada, Consejo Superior de Investigaciones Científicas, Serrano 144, 28006 Madrid, Spain*
(Received 14 March 1997)

Symmetric patterns were recently obtained in the famous Faraday experiment by using a special liquid. A model is developed to explain the robustness of the observed patterns. A dissipation mechanism is introduced phenomenologically and shown to be responsible for the stabilization of patterns with several symmetries. The resulting system of nonlinear equations resembles the well-known Turing equations used to study pattern formation in biological systems. [S1063-651X(97)07810-0]

PACS number(s): 47.35.+i, 47.54.+r, 47.20.Ky

## I. INTRODUCTION

Oscillatory phenomena in nature usually produce spatial or temporal patterns that can be understood theoretically in the framework of parametric resonances. An example of this is the famous Faraday experiment in which surface waves on a liquid are parametrically amplified by forcing a vertical oscillatory motion of the container. The nature of the patterns obtained depends very much on the physical properties of the liquid used, for example, Faraday [1] used water and observed patterns with twofold and fourfold symmetries. Recently, by using highly dissipative systems, patterns with octagonal [2], dodecagonal [3], and pentagonal [4,5] symmetries have been obtained.

The theoretical understanding of this phenomenon was first tackled by Rayleigh [6], who observed that the resonant frequency was different from the frequency of the oscillator. The basic theoretical equations of motion were put forth by Benjamin and Ursell [7], who showed that this hydrodynamic system obeys Mathieu's equation. Extensions of the theory to dissipative viscous fluids have been made recently [8–10].

The solutions of Mathieu's equation in the amplitude-frequency space either diverge or decay exponentially even when linear dissipative terms are included. One way of stabilizing stationary patterns is to consider a nonlinear dissipation mechanism, as we shall show below.

We have repeated the experiments by Torres *et al.* [4,5] using the same special liquid, which has the property of stabilizing fivefold patterns very easily when the height of the fluid is very small compared to the horizontal dimensions, and the frequency of the forcing oscillation is set to 35 Hz. We also obtained practically any $n$-fold symmetric patterns. Some preliminary results on the fivefold patterns have been published recently [11].

We have devised a model for this problem, in which we propose a dissipation mechanism that arises from the interaction of the horizontal component of the velocity field at the bottom of the container with the vertical component. One obtains a set of nonlinear second-order partial differential equations that numerically produces stable patterns with all the observed symmetries. Torres [12] pointed out that the sequence of nonlinear bifurcations in the fivefold experimental patterns resembles the evolutionary sequence of sea urchins. It is suggestive that our equation for the Faraday instability can be written as a set of Turing equations, widely used in morphogenesis and pattern formation in biological problems [13].

In what follows we describe the experiment and show the sequence of patterns obtained by varying the frequency and amplitude. Then we derive the equations for the model and solve them numerically. We also compare several theoretical patterns obtained with their experimental counterparts.

## II. EXPERIMENT

Figure 1 is a sketch of the experimental setup. The experiments described in Refs. [4,5] were reproduced under the same conditions, using fluorinert FC-75 [14] with a 10-cm Petri dish and pouring liquid in it to have a perfectly even layer of width $h_0=2$ mm. The vertical oscillations of the dish were produced with a Brüel–Kjaer 4291 vibrator fed by a high-precision synthesizer that enabled us to change the frequency $\omega$ and amplitude $A$ of the sinusoidal oscillations in a continuous way. The snapshots of the liquid were produced by a video camera attached to the upper part of the setup and using a diffusive screen to enhance the contrast produced by a fiber optics lamp underneath. The amplitude of oscillations has to be increased slowly to produce the instability. This happens when the amplitude is between 40 and 55 $\mu$m. If the

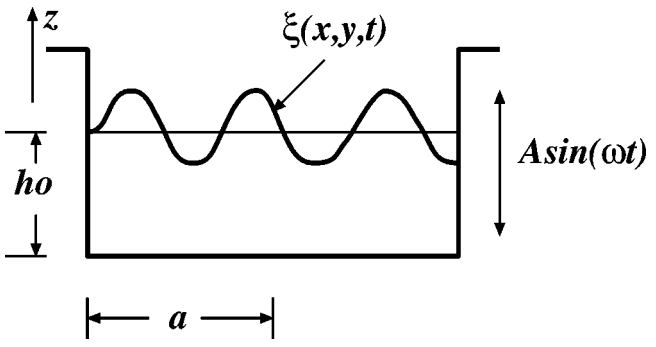


FIG. 1. Experimental setup of the Faraday experiment.

 © 1997 The American Physical Society

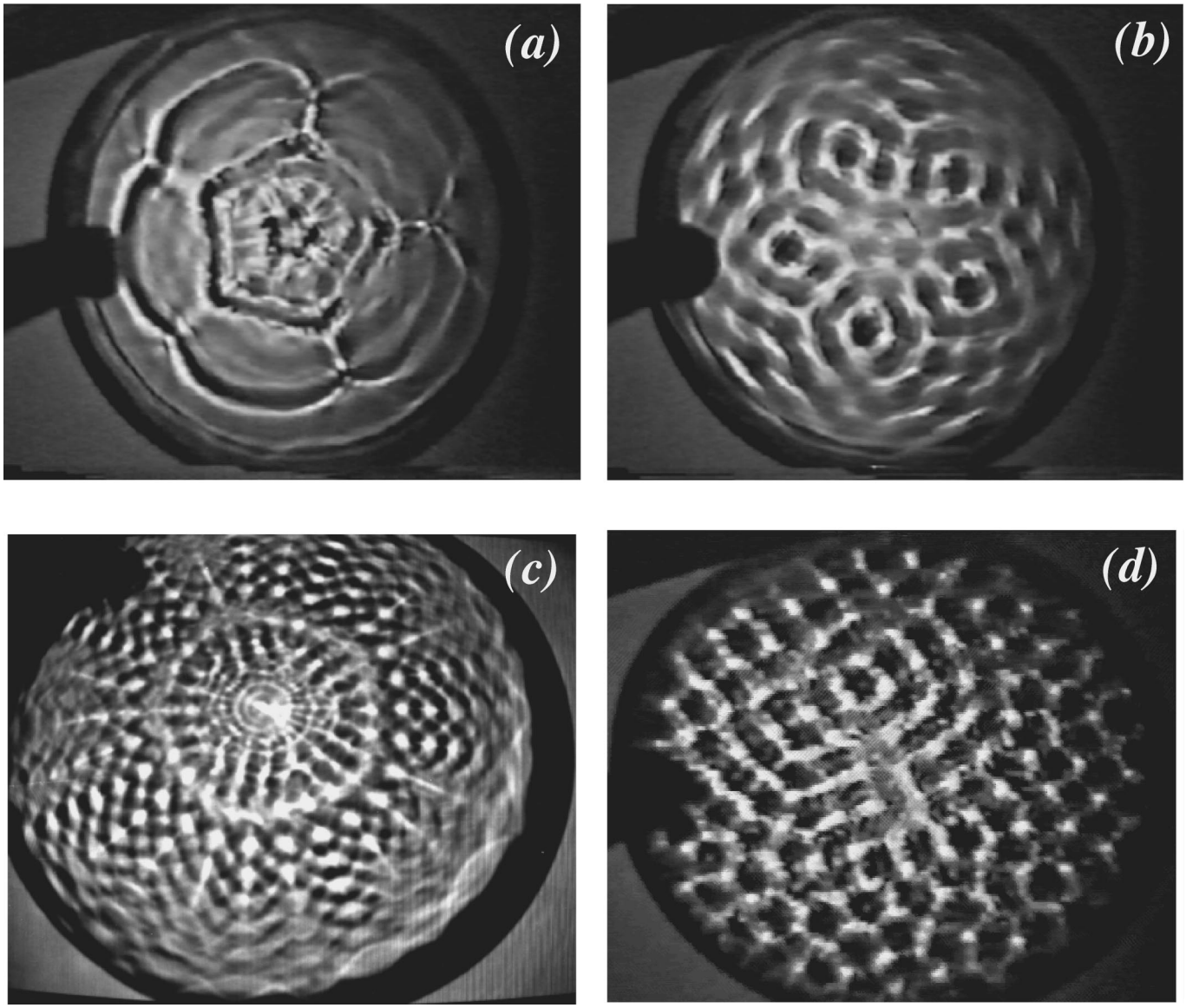


FIG. 2. (a) Fivefold pattern obtained with a frequency $\nu = 8.7$ Hz. (b) Pattern obtained when $\nu = 35$ Hz, and $A = 55$ $\mu$m. (c) Image obtained at $\nu = 35$ Hz and $A = 65$ $\mu$m, averaged over a time of 1 sec (taken from Ref. [4]). (d) Chaotic pattern obtained from (b) when the amplitude exceeds 65 $\mu$m.

amplitude is increased further a chaotic labyrinthine pattern is observed.

In Fig. 2 we show a sequence of experimental patterns with fivefold symmetry, obtained at different points of $(A, \omega)$ space. As pointed out by Torres [12], this sequence of patterns strikingly resembles the shapes of sea urchins in different geological times; for instance, Fig. 2(a) corresponds to the pattern of the oldest fossils of sea urchins, Fig. 2(b) is very similar to the *Hemicidaris intermedia*, who lived about $150 \times 10^6$ years ago, and Fig. 2(c) corresponds to the shape of present time sea urchins. These patterns were obtained by carefully tuning up the appropriate frequency, predicted by the theoretical linearized form of the dispersion relation [see Eq. (1) below]. Figure 2(d) shows a typical chaotic pattern obtained when the amplitude of oscillation exceeds a critical value.

Other types of patterns can be obtained by parametrically exciting other frequencies, for instance, in Fig. 3 we show experimental patterns with eight selected symmetries. In the experiment we were able to find all $n$-fold patterns from $n = 2$ to $n = 21$. Observe that all patterns have a center of symmetry at the midpoint, except the fourfold patterns, which are obtained only when the height of the liquid ($h_0$) is increased. When $h_0$ is very small one is likely to see rolls with $n = 2$.

Observe that these patterns do not correspond to the simple monomodes of the linear regime. These patterns have not always been observed using other liquids. Therefore, it is suggestive that the peculiar physical properties of FC-75 are important in providing the dissipation mechanisms that stabilize patterns with any symmetry. It is worth mentioning that FC-75 is a fully fluored organic liquid that has a very low capillary length ($\approx 0.93$ mm), a low kinematic viscosity $\gamma = 0.8 \times 10^{-2}$ cm$^2$/s, a large density ($\rho = 1.77$ g/cm$^3$), and a high molecular weight ($\mu = 420$).

Unlike the experiments using a glycerol-water mixture [3], the nonlinear dissipation mechanism cannot be attributed to a large dynamic viscosity. In the next section we propose

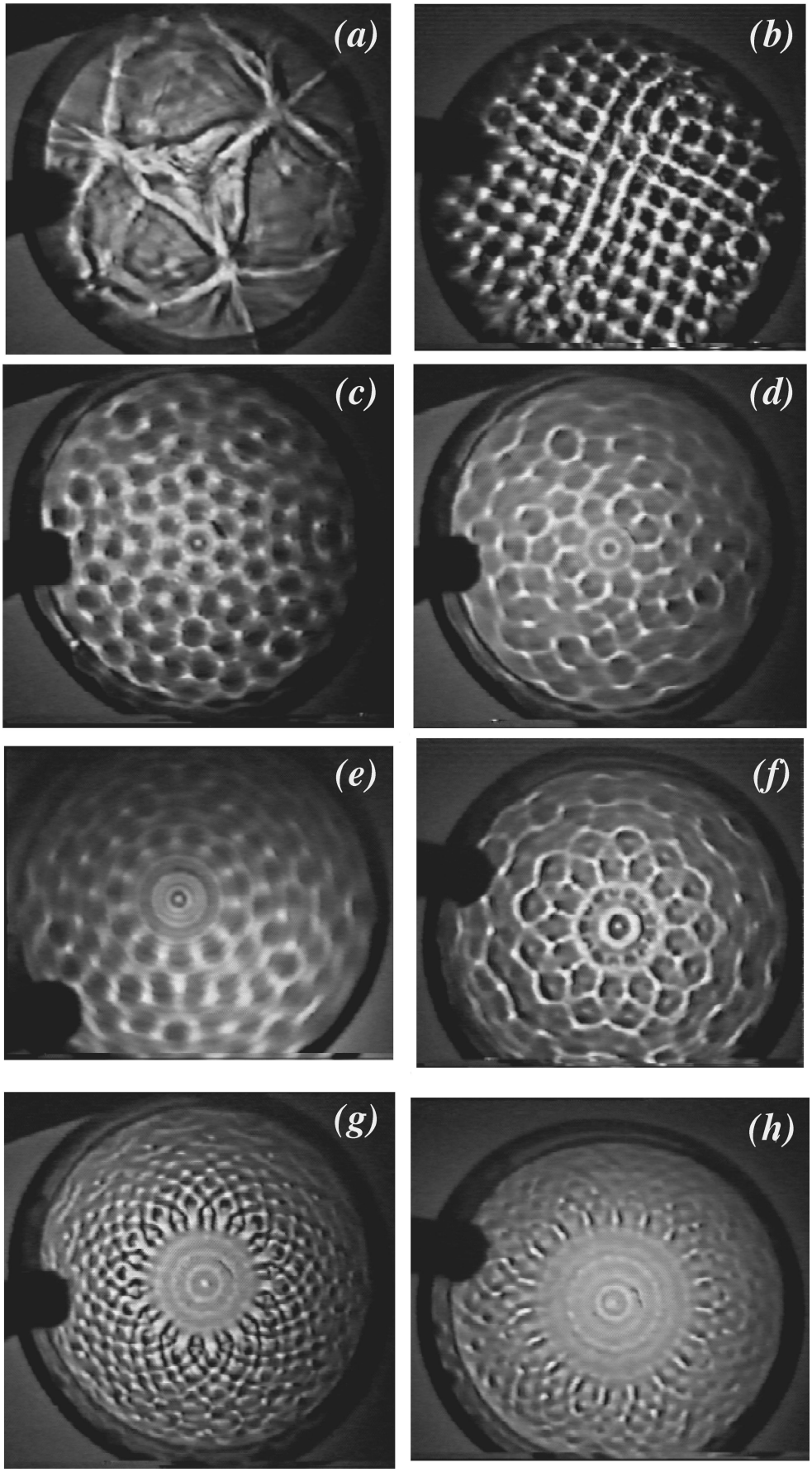


FIG. 3. Sequence of $n$-fold symmetric patterns obtained by increasing the frequency of excitation. (a)–(h) correspond to $n=3$, 4, 6, 8, 11, 13, 14, and 19, respectively.

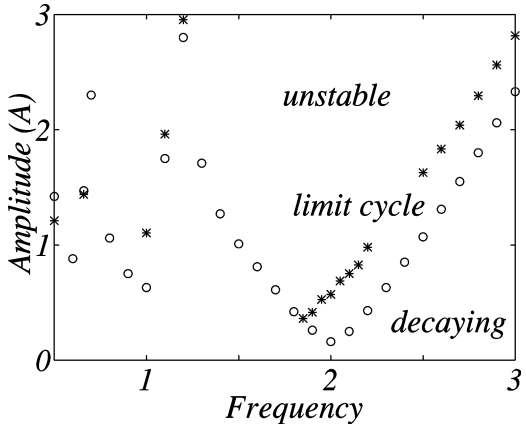


FIG. 4. Resonance tongues of the modified Mathieu's equation. Stability regions are bounded by stars and circles. The amplitude is in units of $h_0$ and the frequency in units of the driving frequency $\omega$.

another dissipation mechanism that takes into account these properties in a phenomenological way.

### III. THEORETICAL MODEL

Our task is to find the shape of the surface $\xi(x,y,t)$ (see Fig. 1) for all points $(x,y)$ at any time $t$. Following numerous former works dealing with the Faraday instability [15,7], one obtains Mathieu's equation for the Fourier components of the potential that defines the velocity field ($\mathbf{v}=-\boldsymbol{\nabla}\phi$). The dispersion relation is

$$\omega_k^2 = k\ \tanh(kh_0)\left[g+\frac{\sigma k^2}{\rho}\right], \tag{1}$$

where $g$ is the vertical acceleration and $\sigma$ is the surface tension. If one systematically neglects terms of order higher than $k^4$ in the dispersion relation, because in the experimental regime $kh_0 \ll 1$, one gets an equation similar to the one derived by Benjamin and Ursell [7], which in the real space representation is

$$\frac{\partial^2\phi}{\partial t^2} = gh_0\left(1-\frac{A}{h_0}\sin\ (\omega t)\right)\nabla^2\phi - \frac{\sigma' h_0}{\rho}\nabla^4\phi, \tag{2}$$

where $\sigma' = \sigma - g\rho h_0^2/3$ is an effective surface tension coefficient. For FC-75 this effective surface tension is zero for a depth of 1.6 mm. Therefore, the experiment is in a regime in which the surface tension term could be neglected. However, as we shall see below, the smallness of this term turns out to be important when comparing our model with a set of reaction-diffusion equations known to produce stable patterns.

This equation has decaying oscillatory solutions or unstable unbounded ones, depending on the values of the two quantities $\omega$ and $A$.

In Fig. 4 the boundaries between the two sorts of solutions are shown by circles. There are no stable patterns.

One needs to consider a mechanism that dissipates energy at the same rate that is fed into the system to obtain stationary patterns. Former theories invoke various sorts of dissipative nonlinear terms in a phenomenological way, frequently appropriate to viscous fluids, which are not fully applicable here. Therefore, we have to introduce alternative mechanisms of dissipation. The usual viscous term when $kh \ll 1$ is [16]

$$\gamma'\nabla^2\frac{\partial\phi}{\partial t}, \tag{3}$$

where $\gamma'$ is a constant related to the kinematic viscosity. This term is used in Ref. [3], and is also obtained in the treatment of a viscous fluid made by Beyer and Friedrich [8] in the appropriate limit. Therefore, we shall include this term in our model (2), although it is not enough to produce stationary patterns.

The fact that the molecular weight $\mu$ is very large implies that there are many internal degrees of freedom that could be used by the liquid to dissipate energy, as it is true in granular systems. In the case of granular convection [17], there is a cross term that couples the horizontal currents with the velocity in the $z$ direction. Therefore, this suggests the inclusion of a term of the form $Rv_z(-h_0)v_x$, where $R$ is a constant strength. This coupling can be phenomenologically modeled by considering the liquid as a group of vertical jets hitting a flat, hard, horizontal surface. The velocity field $v_x$ due to each column can be estimated by considering a two-dimensional laminar flow and using conformal mapping techniques [18]. It is seen that $\partial\phi/\partial x = -C\ \sin(q\phi)$, with $C$ and $q$ constants that are related to the size of the columns (or the size of the molecules). Therefore, we add a term

$$-CA\omega\ \cos\ (\omega t)\ \sin\ (q\phi),$$

to our model (2). The final model equation reads

$$\frac{\partial^2\phi}{\partial t^2} = gh_0\left(1-\frac{A}{h_0}\sin(\omega t)\right)\nabla^2\phi - \frac{\sigma' h_0}{\rho}\nabla^4\phi$$
$$-CA\omega\cos\ (\omega t)\sin(q\phi) + \gamma'\nabla^2\frac{\partial\phi}{\partial t}. \tag{4}$$

The stabilization of the parametrically produced patterns is accomplished by the nonlinear sin term. For small $q\phi$ the leading correction is of the form $q\phi[1-(q\phi)^2/6]$, which is the usual form that gives a limit cycle. The inclusion of a cubic term to stabilize patterns in the Faraday experiment modeling has been studied by Decent and Craik [19]. On the other hand, his term produces an equation similar to the parametric pendulum. To understand this, one could imagine a phenomenology in which a huge molecule traveling downward pushes laterally the other molecules below to make its way through and then the molecules move back when the falling molecule has pass through. This system behaves as a parametric pendulum but, of course, these thoughts have to be tested theoretically in granular systems. Such a study beyond the scope of the present work and is not relevant to the results presented here.

In Fig. 4 we show the stable region for a single-variable parametric pendulum, which is a special case of the above equation. The stable patterns are obtained in the regions between the stars and the circles in Fig. 4.

## IV. EXPERIMENTAL AND THEORETICAL PATTERNS

The solutions of the model (4) neglecting the surface tension term, were explored numerically in parameter space $(A,\omega)$ by a simple Euler method, in a discrete square mesh of sizes $100\times100$ or $200\times200$. The lateral boundary conditions ($\nabla\phi\cdot\mathbf{n}=0$, where $\mathbf{n}$ is the unitary vector normal to the surface) were imposed. The numerical calculation has to be done with care, because the instability and the final pattern depend very much not only on the parameters but also on the initial state.

The best choice for the initial state is to use a linear combination of eigenfunctions of the Helmholtz equation, which are $J_m(\kappa_{mn}r/a)e^{im\theta}$, where $J_m(\kappa_{mn}r/a)$ is a Bessel function of order $m$, whose derivative vanishes at the boundary of the vessel of radius $a$ (see Fig. 1). We used a mixture of $J_0$, $J_3$, and $J_5$, matching the first or second zero of the derivative to the boundary. In the calculations we used the following fixed parameters: $g=h_0=1$, $\gamma'=0.2$, $C=1$, and $q=\omega/2$. In these units $\omega=k$ in the linear regime.

The free variable $A$ has to be tried for each case in order to find the regime of stable patterns; typically this value is $A=0.5$. The other free variable is $\omega$, which gives the symmetry of the pattern obtained. Usually, in our units, its value is very close to twice the $\kappa$ that gives a zero of order $n$ of the derivative of the eigenfunctions of desired symmetry. For instance, to produce a fivefold pattern, $\omega=10.519\,86/a$ since $J_5'(10.519\,86)=0$.

The numerical vessel is not a perfectly circular one; consequently, the initial functions are not the eigenfunctions of the square mesh. Therefore, it is necessary to run the Helmholtz problem ($A=\gamma'=0$) for a while (about 40 000 time steps of 0.1) in order to stabilize the stationary state for the numerical set up. Under these conditions, a pattern of concentric rings is formed, as in the experiment.

Then the appropriate values of $A$ and $\gamma'$ are restored and after $\sim$4000 times steps the perfectly circular symmetry of the stationary pattern breaks and some bumps appear, just as it is seen in the experiment. Figure 5 shows the numerical calculation at this stage and its comparison with the experiment under the same conditions.

It was observed that once an $n$-fold pattern had settled down, it remained unchanged for as many as 100 000 iterations. Figure 6 shows a stable ten-fold pattern obtained with a typical calculation and compares it with an experimental image with the same symmetry. Observe that the appearance of both is very similar, although not identical. This is to be expected since the experimental image is the result of very complicated optical phenomena, while the theoretical image is constructed by assigning a linear scale of grays to the heights of the liquid.

When the amplitude $A$ is increased beyond a certain value, in either the experiment or the calculation, some typical labyrinthine patterns are observed. These are shown in Fig. 7.

In the experiments, these chaotic patterns retain some of the symmetry of the pattern that originated them, and if the amplitude is diminished slowly, the former symmetric pattern is recovered. In this regime of high amplitude some averaged symmetric and complicated images, which correspond to the second instability onset, are obtained [see Fig. 2(c)].

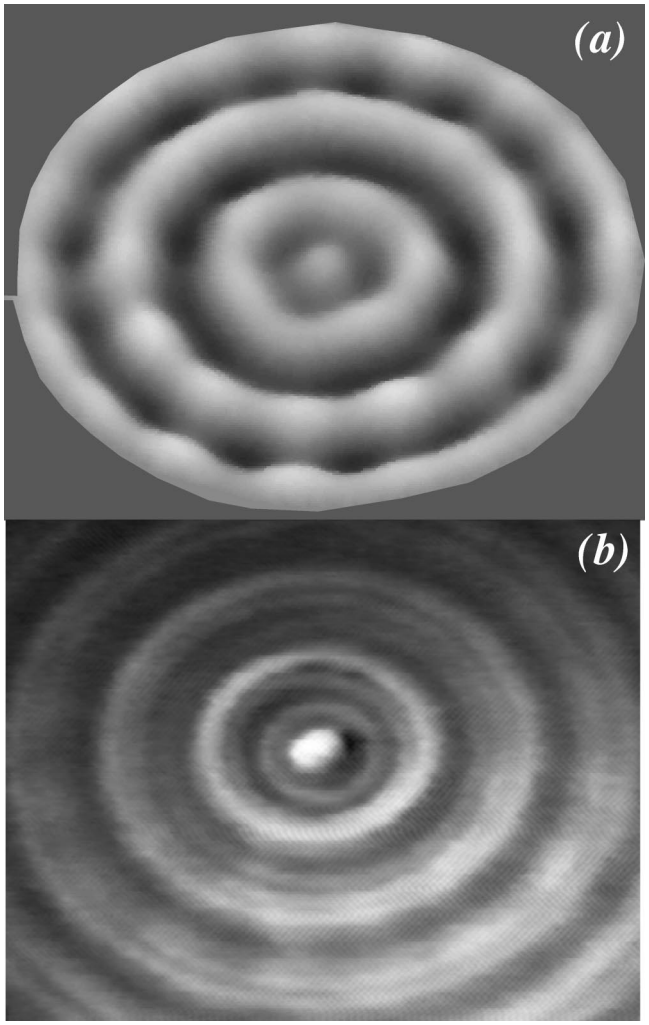


FIG. 5. (a) Image of the shape of the surface in a numerical calculation shown exactly after the symmetry breaking. The frequency of excitation was appropriate for stabilizing fivefold patterns. (b) Photograph of the experimental vessel taken just before the pattern shown in Fig. 2(b) was settled.

In Fig. 8 we show a typical calculation to mimic the second instability. In Fig. 8(a) we show the time history of the central point in the mesh around the time when the second instability appears (after $\sim$560 iterations). The amplitude of the forcing vibration was set to 3/2 the one that produced the first symmetry breaking, which produces an image like the one shown in Fig. 8(b). One can notice that the oscillation in this situation has mainly one Fourier component that corresponds to the external driving oscillation, although there is a wide band of frequencies around it, as shown in Fig. 8(c) with a continuous line. This plot was obtained by performing a fast Fourier transform in the interval 20–560 iterations. In the same figure, the dotted line corresponds to the Fourier transform taken in the interval 560–2000 iterations. Notice that many frequencies are amplified, in particular the ones that correspond to the first and second parametric resonances, of the form $\omega(k)=2\omega/n$. The image produced after the second instability is shown in Fig. 8(d). Observe that the main symmetries present are threefold and tenfold, just as

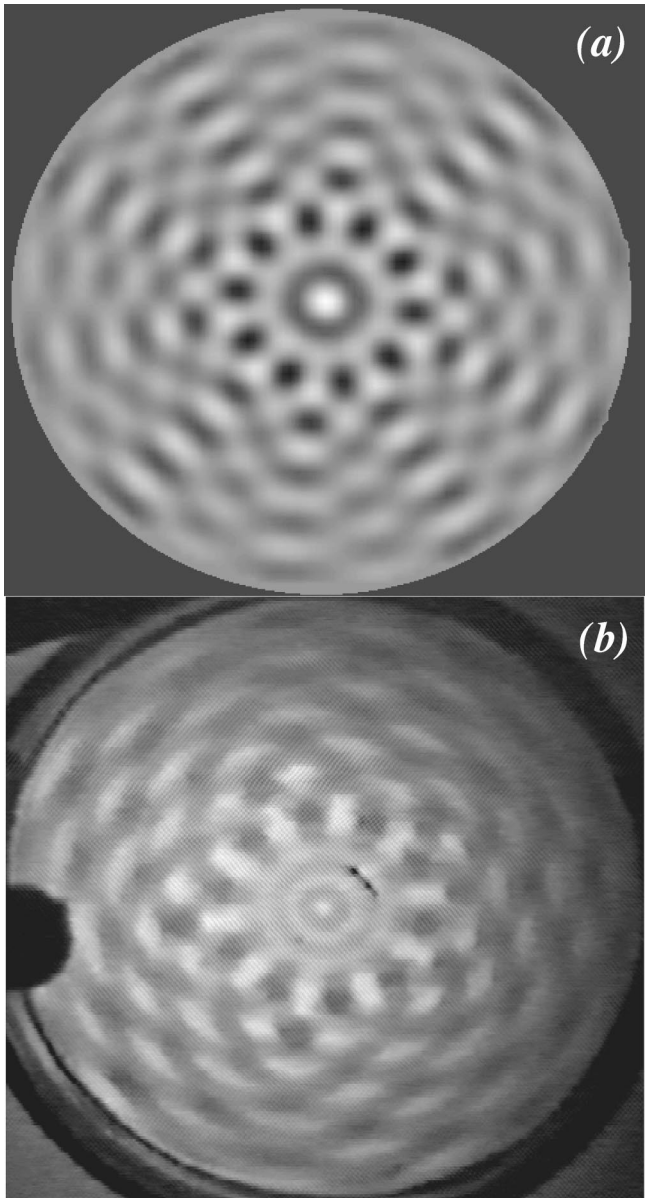


FIG. 6. (a) Image of the shape of the surface in a numerical calculation where a stable tenfold pattern is observed. (b) Photograph of the experimental vessel showing a stable tenfold pattern.

the pattern that originated it, but in a rather complicated way. See also the presence of threefold symmetry at the center of Fig. 2(b).

A quantitative comparison between the experimental patterns and the calculated ones can be done by means of a Fourier-Bessel analysis. However, there are serious difficulties in doing this because the experimental images are the result of a very complicated optical effect that has to be precisely modeled before any attempt to compare images that the eye can discern as similar. This study is currently being carried out.

We noticed by Fourier-Bessel analysis of the calculated images that at medium ranges of $A$ the tongues, like the ones shown in Fig. 4, are wider for threefold and sevenfold symmetries. In the experiments the five-fold patterns are extremely robust at $\nu=35$ Hz provided that the fluid height is exactly set at $h_0=2$ mm. For slightly lower values threefold symmetry was dominant, and for higher values a square pattern was obtained, as observed in experiments [20]. At exceedingly high values of $A$ the fluid develops fingers that eventually splash in the experiment, in the simulations a localized instability appears usually at one edge of the vessel [see the bottom of Fig. 7(a), where an extremely high contrast region shows the onset of a localized instability], in a fashion similar to the localized instabilities found experimentally by Lioubashevski *et al.* [21].

## V. ANALOGY WITH TURING SYSTEMS

In this section we would like to stress and analyze the point already made by Torres [12], and illustrated in Fig. 2. It is remarkable that the five-fold patterns in the Faraday experiment resemble very much the shapes found in the evolutionary development of the shell of sea urchins. Without pretending to make any conclusions concerning the particular biological or chemical mechanism involved in such a complicated process as the evolution of living creatures, we shall analyze the model (4) to make a connection with the kind of nonlinear reaction-diffusion equations currently used to mimic patterns in living organisms.

If one defines

$$\psi=\dot{\phi}+\beta\phi+\alpha\nabla^2\phi,$$

where $\alpha=\frac{1}{2}(-\gamma'\pm\sqrt{\gamma'^2-4\sigma' h_0/\rho})$ and $\beta=g h_0[1-(A/h_0)\sin(\omega t)]/(2\alpha+\gamma')$, one can write the second-order equation (4) as the system

$$\dot{\phi}=(\psi-\beta\phi)-\alpha\nabla^2\phi, \tag{5}$$

$$\dot{\psi}=[\beta(\psi-\beta\phi)+C\ \sin(q\phi)]+(\alpha+\gamma')\nabla^2\psi, \tag{6}$$

which is a set of Turing equations [22]. For small effective surface tension one of the *diffusion coefficients* is much smaller than the other, a condition usually met in modeling biological patterns from morphogens. Observe that the diffusion coefficients could be complex if $\gamma'^2<4\sigma' h_0/\rho$. Using the experimental values for the physical constants in the experiment of Refs. [4,5], from the equation for $\alpha$ one obtains real diffusion coefficients if $h_0\geqslant 1.6$ mm and complex otherwise. It is remarkable to notice that the liquid height used in the experiments is very close to this critical value, which allows one to neglect the surface tension term, but still gives a real diffusion coefficient.

Obviously, this is not the only way of defining a set of reaction-diffusion equations compatible with our model. The external driving force could be considered as another chemical species that oscillates harmonically in time with natural frequency $2\omega$, in which case one ends up with a set of four coupled nonlinear equations.

Turing systems have been widely treated numerically and the different kinds of patterns obtained can be classified roughly as spots or stripes, depending on the point in parameter space one is interested. These calculations usually refer to systems with periodic boundary conditions. We have studied different Turing systems in confined regions [23], where a richer variety of spatial patterns can be produced if one modifies the sources at the boundaries. However, the patterns

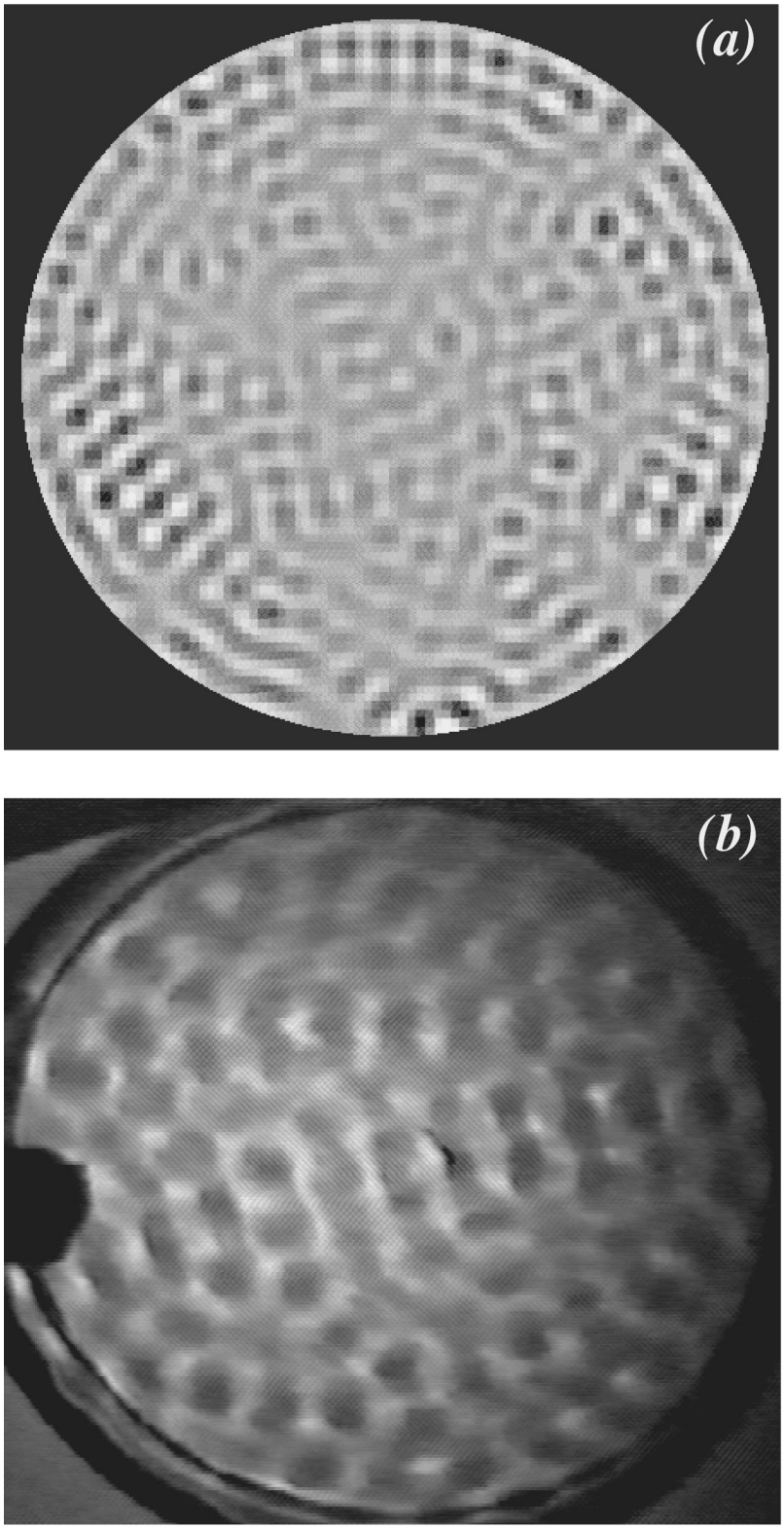


FIG. 7. (a) Numerical calculation in the situation when $A=0.9$. Observe the chaotic structure. (b) Photograph of the experimental vessel showing a chaotic pattern.

are not produced by interference of monomodes imposed by the boundary, but they are truly nonlinear. Patterns in confined Turing systems are affected by the shape of the boundaries mainly by orientating them and creating ''crystalline defects.''

The role of the shape of the boundary can be negligible in the Faraday experiment in two cases: Either the dynamic viscosity of the liquid is very large [3,10] or the size of the cells is small compared to the size of the vessel. The fact that in our model there is a dissipation mechanism different from the viscosity term and that it allows one to make a connection with reaction-diffusion systems allows one to assert that

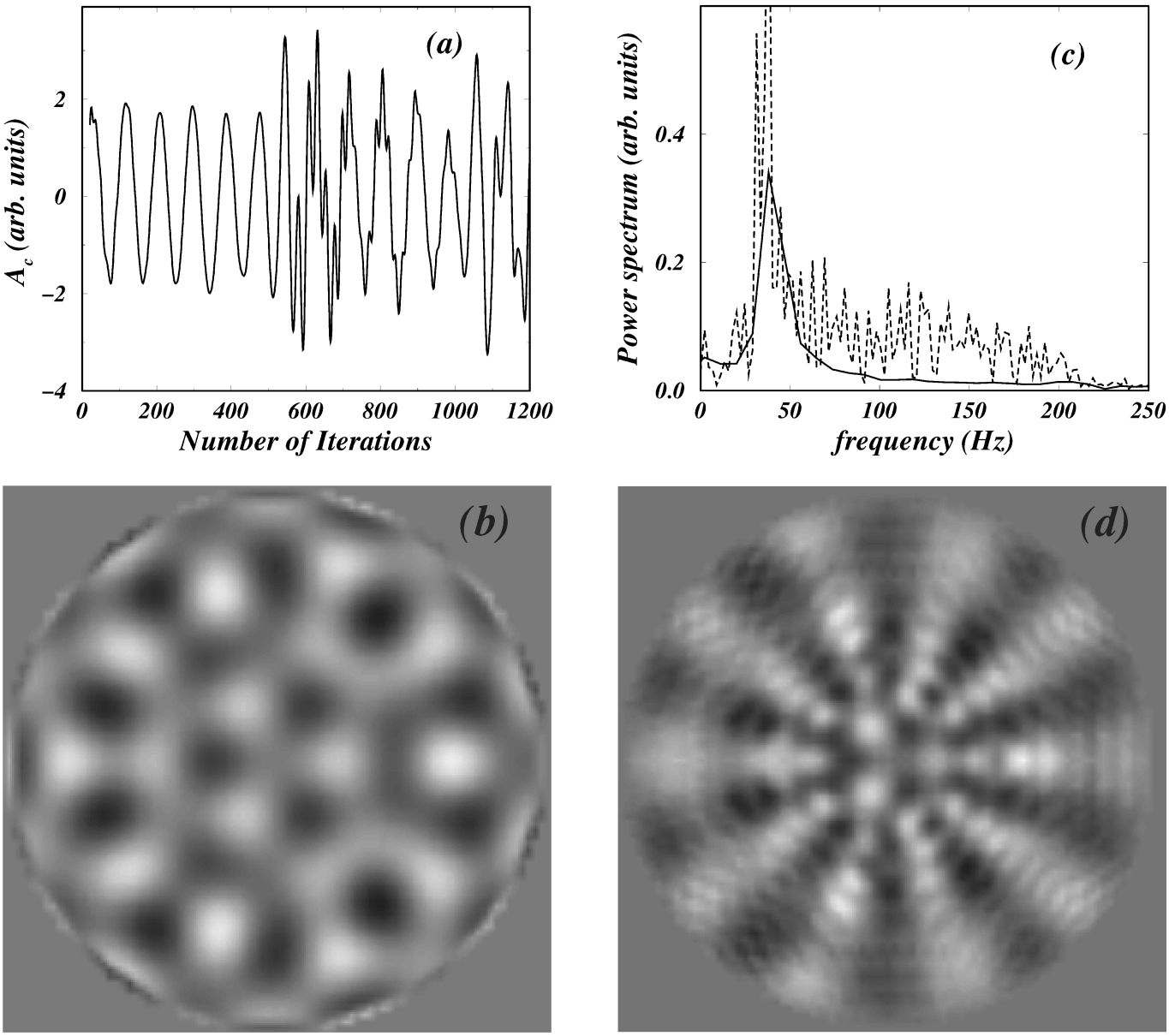


FIG. 8. (a) Amplitude of the central point in the mesh ($A_c$) as a function of time, when it is driven at $\nu = 37$ Hz and $A = 0.75$. (b) Image corresponding to iteration 50. (c) Power spectrum obtained by fast Fourier transforming (a). The continuous line is obtained from iteration 20 to 560 and the dotted line is obtained from iteration 560 to 2000. (d) Image corresponding to iteration 1200.

the patterns observed are reflecting truly nonlinear behavior. Binks and van de Water [24] have found a series of increasing rotational symmetry patterns using a liquid with very low viscosity and surface tension. They show that these patterns are truly nonlinear and that the effects of the boundary are small. In our case the cell size is small compared to the vessel dimensions in almost all the cases. Therefore, we can assert that at least here the boundary is not important. In the case of the large cells of Figs. 2(a) and 3(a), a Fourier-Bessel analysis shows that there are many frequencies of the type $2\omega/n$ that are parametrically enhanced and the onset of the instability behaves as a truly nonlinear bifurcation.

Reaction-diffusion equations have been used to model symmetry-breaking patterns in other completely different systems; for example, Gunaratne *et al.* [25] have found patterns in cellular flames and used a set of diffusion equations that are strikingly similar to our Eq. (6) except that the nonlinear coupling is cubic instead of the sin term and the nonvariational gradient square terms that produce rotating modes in their flames are not present in our model.

## VI. CONCLUSION

In this paper we have analyzed the fascinating problem of the Faraday instability both experimentally and theoretically. We have found that for certain liquids, in which viscosity is very small and with peculiar physical properties such as a high molecular weight and density, there exists an additional dissipation mechanism that introduces an important nonlinear term in the equations of motion. This mechanism produces the stabilization of symmetric patterns. The model equation was solved numerically and the patterns produced were analyzed and compared with experimental images. The agreement seems to be satisfactory to the point that some

experimental patterns were first predicted by the simulations and then found in the experiments.

It is remarkable that the model equation can be written as a Turing system with the possibility of having complex diffusion coefficients. The study of Turing systems with complex diffusion coefficients in confined regions is currently being carried out.

There is still much to be learned about this system, and the quantitative analysis of the nonlinear phenomena is still missing. This shall be the matter of a future work.

## ACKNOWLEDGMENTS

We are thankful to UNAM DGAPA, Projects Nos. IN104296 and IN107296, and CONACyT, Projects Nos. 0088P-E and 2677P-E, for financial support. R. A. B. thanks the Program CONACyT-CSIC (Spain), Project No. E130-1331, for the hospitality in Madrid, where a substantial part of this work was carried out.

[1] M. Faraday, Philos. Trans. R. Soc. London **121**, 299 (1831).
[2] B. Christiansen, P. Alstrom, and M. T. Levinsen, Phys. Rev. Lett. **68**, 2157 (1992).
[3] S. Fauve, in *Dynamics of Nonlinear and Disordered Systems*, edited by G. Martinez-Mekler and T. H. Seligman (World Scientific, Singapore, 1995), p. 67.
[4] M. Torres, G. Pastor, I. Jimenez, and F. Montero de Espinosa, in *Proceedings of the Fifth International Conferences on Quasicrystals*, edited by C. Janot and R. Mosseri (World Scientific, Singapore, 1995), p. 257.
[5] M. Torres, G. Pastor, I. Jimenez, and F. Montero de Espinosa, Chaos Solitons Fractals **5**, 2089 (1995).
[6] Lord Rayleigh, Philos. Mag. **15**, 229 (1883); **15**, 285 (1883); **16**, 50 (1883).
[7] T. B Benjamin and F. Ursell, Proc. R. Soc. London, Ser. A **225**, 505 (1954).
[8] J. Beyer and R. Friedrich, Phys. Rev. E **51**, 1162 (1995).
[9] E. Cerda and E. Tirapegui, Phys. Rev. Lett. **78**, 859 (1997).
[10] K. Kumar and L. S. Tuckerman, J. Fluid Mech. **279**, 49 (1994).
[11] R. A. Barrio, J. L. Aragón, C. Varea, M. Torres, I. Jimenez, and F. Montero de Espinosa, in *Proceedings of the Second World Congress of Non-Linear Analysis, Athens, 1996* (Elsevier, Kidlington, in press).
[12] M. Torres (unpublished).
[13] J. D. Murray, *Mathematical Biology* (Springer-Verlag, Berlin, 1993); R. Dillon, P. K. Maini, and H. G. Othmer, J. Math. Biol. **32**, 345 (1994).
[14] This product was kindly donated by the 3M Company of Minnesota.
[15] J. W. Miles and D. Henderson, Annu. Rev. Fluid Mech. **22**, 143 (1990).
[16] L. D. Landau and E. M. Lifshitz, *Fluid Mechanics* (Addison-Wesley, Reading, MA, 1968), p. 100.
[17] H. Hayakawa, S. Yue, and D. C. Hong, Phys. Rev. Lett. **75**, 2328 (1995).
[18] Z. Nehari, *Conformal Mapping* (Dover, New York, 1975), p. 195.
[19] S. P. Decent and A. D. D. Craik, J. Fluid Mech. **293**, 237 (1995).
[20] K. Kumar and K. M. S. Bajaj, Phys. Rev. E **52**, R4606 (1995).
[21] O. Liouvashevski, H. Arbell, and J. Fineberg, Phys. Rev. Lett. **76**, 3959 (1996).
[22] A. M. Turing, Philos. Trans. R. Soc. London, Ser. B **237**, 37 (1952).
[23] C. Varea, J. L. Aragón, and R. Barrio, Phys. Rev. E **56**, 1250 (1997).
[24] D. Binks and W. van de Water, Phys. Rev. Lett. **78**, 4043 (1997).
[25] G. H. Gunaratne, M. El-Hamdi, M. Gorman, and K. A. Robbins, Mod. Phys. Lett. B **10**, 1379 (1996).